PHYSICAL REVIEW C, VOLUME 60, 014906

Two-body Bose-Einstein correlations in simulated relativistic heavy ion collision events

R. L. Ray and G. W. Hoffmann
Department of Physics, The University of Texas at Austin, Austin, Texas 78712
(Received 10 March 1999; published 18 June 1999)

An algorithm for generating Bose-Einstein momentum space correlations in the particle distributions of simulated relativistic heavy-ion collision events is extended for applications to experiments at the Relativistic Heavy Ion Collider. Quality fits to the momentum space correlations for spherical and nonspherical source geometries are obtained for both the like charged pion $[(\pi^+\pi^+)$ and $(\pi^-\pi^-)]$ and unlike charged pion $(\pi^+\pi^-)$ two-body distributions predicted for 200*A* GeV Au+Au central collisions. The momentum space correlations not directly constrained in the fitting algorithm are examined, and strong correlations are found for both the like and unlike charged pion spectra indicating that the correlation signals generated by the algorithm are robust. The model is well suited for the simulation needs of present and future heavy-ion experiments.
[S0556-2813(99)04807-4]

PACS number(s): 25.75.Gz, 24.10.Lx

I. INTRODUCTION

In the near future the Relativistic Heavy Ion Collider (RHIC) at the Brookhaven National Laboratory (BNL) and the four accompanying detectors will begin new studies of dense hadronic matter at unprecedented high temperatures and energy densities. The primary goals of the RHIC program are to search for evidence of long-range color deconfinement and chiral symmetry restoration in the states of the system. Important to these studies is the determination of the phase space distribution and time evolution of the collision region via energy-momentum space correlation analyses. The analytical techniques are based on the well-known Hanbury Brown–Twiss (HBT) quantum interference mechanism which occurs among the outgoing, identical particles from the collision region or incoherent ''source'' [1]. Recent work suggests that the time evolution of the hot, expanding collision region carries one of the more robust signals of color deconfinement and possible quark-gluon plasma (QGP) formation [2]. Accurate determination of the one- and two-body energy-momentum space distributions is therefore crucial to the physics goals of the RHIC project.

Unfortunately, a number of dynamical and experimental effects tend to obscure the relation between the measured correlations in momentum space and the underlying distribution and time evolution of the collision region or ''source.'' The dynamical effects include those due to the Coulomb interaction [3], final state hadronic scattering and resonances [4–6], and many-body symmetrization [7,8]. Experimental effects include finite momentum resolution, two-track resolution, finite detector acceptance, tracking efficiency and purity, track splitting, and particle identification efficiency and contamination.

The intent of the present work is to develop a new simulation tool which can be used to study quantitatively the differences between the two-body energy-momentum space distributions at macroscopic distances from the collision region and those obtained directly from the detector-event reconstruction system. This work presents an algorithm and computational model which permit two-body energy-momentum space correlations to be imposed on the particle distributions predicted by relativistic heavy-ion collision event generators [9,10]. Comparison of input correlations with those deduced after passing the simulated events through detector simulation, reconstruction and correlation analysis software, provides a quantitative measure of the intervening experimental effects. Of course the quality of this determination depends upon that of the detector simulation — an important but separate issue which is not addressed here.

The model described in Ref. [11] was extended to accommodate the high multiplicity events expected at RHIC, to permit two-body correlations to be generated simultaneously for as many as two particle types, to include three-dimensional correlation functions representing nonspherical source geometries, to include more realistic correlation models as well as realistic Coulomb corrections appropriate for finite source sizes, and to be applicable to the output from standard heavy-ion collision event generators. The two-body momentum space correlation function is six dimensional [3,4], whereas for the present model this quantity is only constrained with respect to one or three coordinates. The extent to which the model provides two-body correlations with respect to the other, unconstrained coordinates is also studied. Such correlations are found to be of reasonable strength and range. Given these additional features the HBT correlation processing model presented here is well suited for the simulation needs of the RHIC experiments.

A presentation of the algorithm and model is given in Sec. II. Section III gives the results of an application to RHIC events. The study of unconstrained correlations is presented in Sec. IV. Finally, a summary and some conclusions are presented in Sec. V.

II. CORRELATION ALGORITHM AND MODEL

Algorithms. The basic method for producing correlations of a specified form in the two-body relative momentum distributions of simulated RHIC-like events was described in Ref. [11] and is essentially a specific application of the more general Metropolis *et al.* [12] method. Briefly, the steps in this algorithm are (1) the three-momentum vector of one of

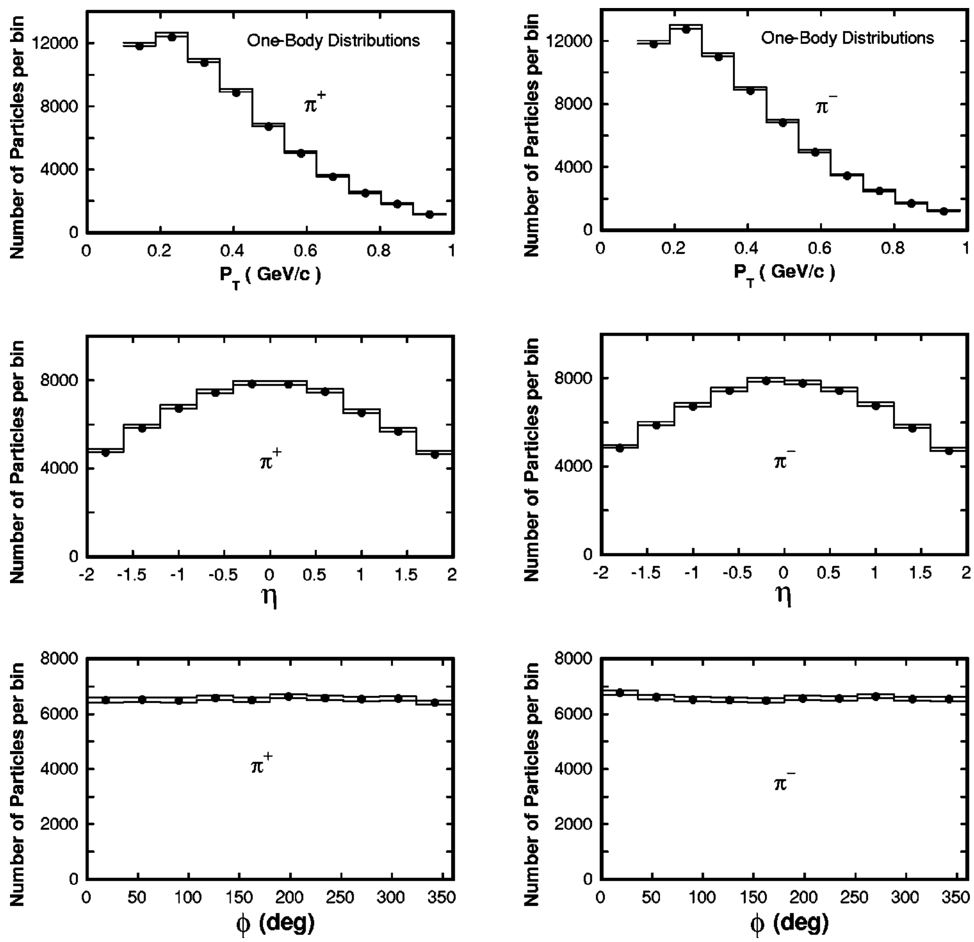

FIG. 1. One-body π^+ and π^- inclusive distributions with respect to p_T, η (pseudorapidity), and ϕ (azimuthal angle) for 25 VENUS-like RHIC energy Au+Au central collision events. The reference and fitted distributions are shown by the solid lines and solid dots, respectively. The errors shown are statistical only; errors smaller than the data symbols are not shown.

the accepted particles is randomly shifted within a confined range of ~ 100 MeV/c, (2) the resulting one- and two-body distributions are calculated and compared with reference and model values using a chi-square method, (3) if the resulting distributions are in better agreement with the reference and model values (i.e., lower chi-square), then the shifted momentum is retained, if not, then the particle's momentum is restored to the original value, (4) steps (1) – (3) are repeated for each accepted particle, in random order, and (5) the entire process, steps (1) – (4), is repeated until satisfactory agreement with the reference and model values is achieved. For the cases studied here about 15 – 30 iterations were required to achieve excellent fits to the one-body reference distributions and the various two-body correlation models.

Other approaches exist for simulating momentum space correlations in the particle distributions resulting from high energy heavy ion collisions. In the method of Pratt *et al.* [13] the particle momenta are not altered. Instead the number of particle pairs in each relative momentum bin is weighted according to the required correlation model. In other words, the ''correlations'' are introduced *after* the detector simulation and event reconstruction analyses are completed, thus not actually testing the overall detector-software performance for events with enhanced numbers of close track pairs.

A different approach [14], incorporated into the event generator PYTHIA [15], does involve shifting the particle momenta. The shifts are calculated for each particle pair in an uncorrelated event such that the relative momentum magnitude is reduced for each pair, but in a way such that larger shifts result for pairs with smaller relative momentum. The vector sum of all such shifts from all pairs for each particle determines the net momentum change for that particle. The algorithm rigorously conserves three-momentum but not energy (or vice versa). It was applied to one-dimensional π^- correlations for heavy-ion collisions in Ref. [16].

Others [17,18] have applied the Metropolis *et al.* method [12] to the problem of determining the many-body ($n \geqslant 2$) symmetrization effects on the observed one- and two-body distributions. Many-body correlated particle distributions were produced using Monte Carlo methods. These approaches are generally impractical for high multiplicity RHIC-type events.

In Ref. [7] a practical, analytical method was developed for computing the many-body symmetrization corrections to the observed one-body distributions for arbitrary (non-

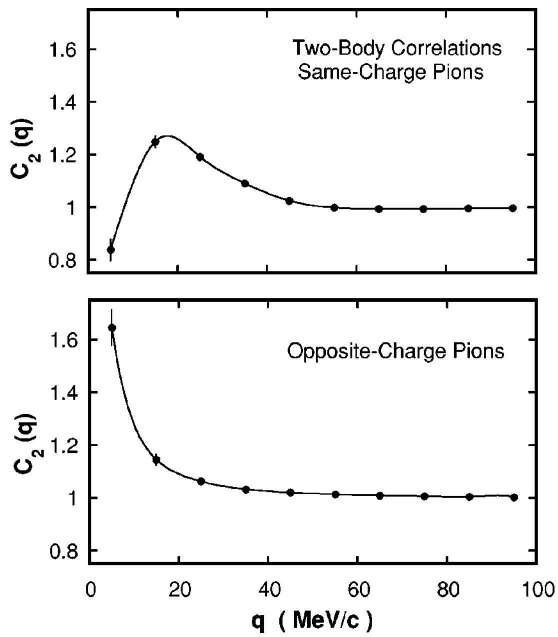

FIG. 2. Inclusive fits (solid dots) to the like charged pion (upper panel) and unlike charged pion (lower panel) two-body, one-dimensional correlation model values (solid lines). Statistical uncertainties in the fitted values are indicated by the error bars if larger than the data symbols.

Gaussian) source functions. It is straightforward to extend these calculations to include two-body distributions and two-body correlations. Also, analytical methods have been presented for Gaussian sources [8]. For the present work it was assumed that many-body symmetrization effects on the one- and two-body distributions can be taken into account separately. The Monte Carlo methods described here may then be used to generate simulated events which display the specified one-body distributions and two-body correlations which are appropriate at macroscopic distances from the source.

Model. In general, the one-body distributions predicted by standard event generators are fully three dimensional, depending arbitrarily on p_T (transverse momentum), η (pseudorapidity), and ϕ (azimuthal angle). However, even for RHIC events, the one-body distributions cannot be binned into a reasonable three-dimensional grid with ample statistics. Instead, for all particles within the specified kinematic acceptance range the momentum vectors were projected onto independent p_T, η, and ϕ axes, and the one-body distributions were binned accordingly. The track adjustment procedure was constrained (via a chi-square fitting procedure described in the following) such that these one-body projected distributions were reasonably maintained throughout the fitting procedure with respect to reference distributions. It is worthwhile to note that, although the present algorithm does not explicitly conserve the overall total momentum and energy of the accepted particles in the event, the chi-square fitting procedure for the projected one-body distributions does, in effect, constrain the original total momentum and energy.

The two-body correlations were computed in the standard way according to

$$C_2(\boldsymbol{p}_1,\boldsymbol{p}_2)=\frac{N_2^{(B)}}{N_2^{(S)}}\frac{S_2(\boldsymbol{p}_1,\boldsymbol{p}_2)}{B_2(\boldsymbol{p}_1,\boldsymbol{p}_2)}, \tag{1}$$

where $S_2(\boldsymbol{p}_1,\boldsymbol{p}_2)$ and $B_2(\boldsymbol{p}_1,\boldsymbol{p}_2)$ are the correlated and uncorrelated two-body momentum space spectra, respectively, for particle pairs with momenta $\boldsymbol{p}_1$ and $\boldsymbol{p}_2$, and $N_2^{(B)}$ $(N_2^{(S)})$ is the number of particle pairs in the uncorrelated (correlated) set of particles. The particle pair spectra were binned into either one- or three-dimensional grids depending on the choice of correlation models discussed in the following. In this work we have assumed a one-dimensional, three-dimensional Bertsch-Pratt (BP) [19], or three-dimensional Yano-Koonin-Podgoretskiĭ (YKP) [20] correlation model.

The one- and two-body reference distributions were obtained from the set of input events which are assumed to be physically similar and only differ statistically from one another. The one-body p_T, η, and ϕ projected reference distributions were calculated from the inclusive sum of particles in the entire sample of events. The two-body reference distribution, B_2 in Eq. (1), was generated from particle pairs obtained by mixing particles from different events which lie within the overall acceptance. Pairs were formed by mixing particles from events 1 and 2, then adding pairs from events 2 and 3, and so on until all consecutive event pairs were used. For RHIC-like events only a few tens of event pairs are required in order to achieve sufficient statistical accuracies for the one- and three-dimensional two-body distributions. For the calculations presented here, twenty five Au+Au central 200*A* GeV VENUS-like events [10] were used. The statistical uncertainty in the two-body, one-dimensional (three-dimensional BP) reference distribution for the low relative momentum bins was typically 1% (about 2%) or less. The statistical errors for the YKP reference distribution at low relative momenta varied typically from about 2–5 %. A few bins for the YKP form were too sparsely populated to be useful in the fitting procedure.

The track momentum shifts were constrained by the total chi-square computed for the one-body distributions and the one- or three-dimensional correlation function. The chi-square values for the one-body distributions (different particle types were treated separately) were obtained using the binned p_T, η, and ϕ projected distributions for the event, the binned reference distributions described above (normalized to the total number of accepted particles in the event), and the statistical errors for both distributions (combined in quadrature). The chi-square values for the correlation functions were obtained using the binned quantity in Eq. (1), the specified analytical model values at the centers of each bin, and the statistical errors in C_2 from Eq. (1). Weighting factors were used to combine the chi-square values for the one-body distributions for both particle types and the chi-square values for the correlation functions for both like and unlike particle pairs. Equal weighting factors were used for the chi-square values for each of the one-body distributions as well as for the selected two-body correlation functions. The chi-square values for the latter quantity were either that for the

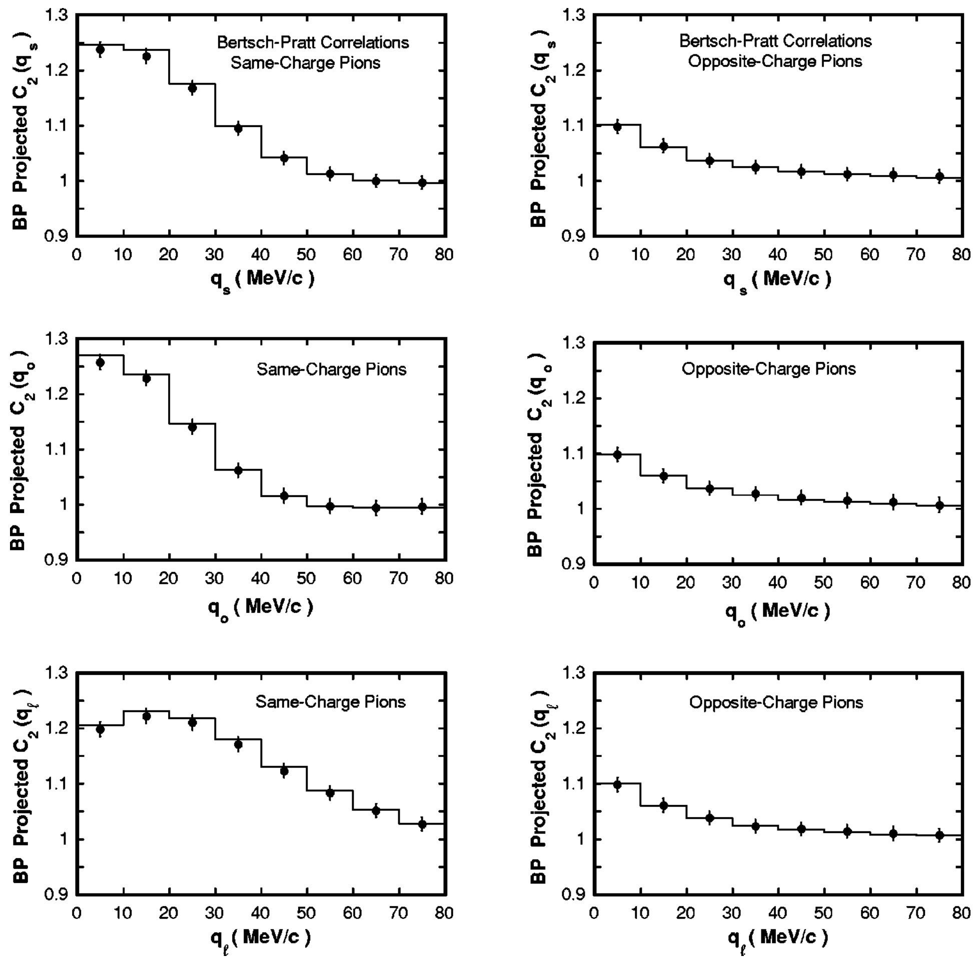

FIG. 3. Inclusive fits (solid dots) to the projected Bertsch-Pratt side-out-longitudinal parametrization of the two-body correlation function (solid lines). Results for the like and unlike charged pion pairs are shown in the left and right set of panels, respectively. Statistical uncertainties in the fitted values are indicated by the error bars if larger than the data symbols.

one-dimensional, or the three-dimensional BP form, or the YKP model. No attempt was made to simultaneously fit two or more correlation models.

New capabilities of the model. The computational requirements of the correlation method in Ref. [11] are too demanding for the multiplicities predicted for Au+Au central collision RHIC events. Calculations [9,10] suggest that of order 5000 charged particles (mainly pions) may be produced in each Au+Au central collision within the acceptance of the STAR (Solenoidal Tracker at RHIC) detector [21]. In order to accommodate the large number of identical particles per event, the one-body momentum space distribution was subdivided into sectors in p_x, p_y, and p_z (z axis along beam direction). Only pairs of particles within the same sector or pairs in which the two particles are in separate, but neighboring sectors were included in the calculations. The sector dimension (typically 100 MeV/c along each axis) was chosen to be somewhat larger than the correlation range such that no particle pairs in the important relative momentum range were lost. This procedure drastically reduced the number of pairs for which kinematic calculations were needed and reduced the computational demand tremendously. On the other hand, a substantial amount of particle-sector ‘‘bookkeeping’’ is now required in the computer code.

Recent HBT studies of Pb+Pb 158A GeV fixed target data from NA49 (CERN) [22] demonstrated the importance of simultaneous analysis of $\pi^+\pi^+$, $\pi^-\pi^-$, and $\pi^+\pi^-$ correlations. Detailed study of the $\pi^+\pi^-$ Coulomb correlation reveals quantitative information about the source size and provides empirical corrections that can be used directly in analyses of the like charge correlations to accurately ‘‘subtract’’ the repulsive Coulomb contribution. Therefore, the simulation model [11] was extended to include particle momentum adjustments for up to two particle types (e.g., π^+ and π^-) during each iteration. The chi-square constraints on the fitting were applied to both the like and unlike particle pair correlations.

For the results presented here the following analytical model was taken for C_2:

$$C_{2,\mathrm{model}} = G_{\mathrm{Coul}}[1+\lambda b^2], \tag{2}$$

where G_{Coul} is the Coulomb correction factor, λ is the chaoticity parameter, and the function b was taken to be one of the following forms;

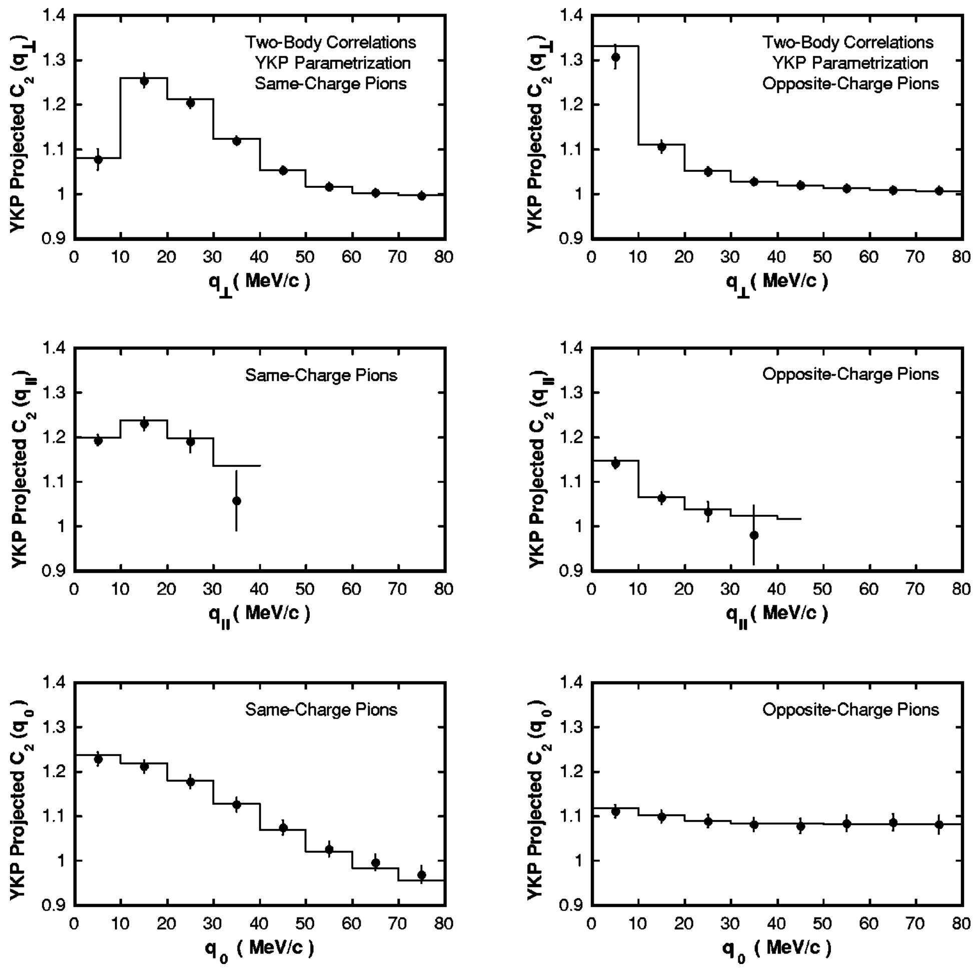

FIG. 4. Inclusive fits (solid dots) to the projected perpendicular-parallel-emission time YKP parametrization of the two-body correlation function (solid lines). Results for the like and unlike charged pion pairs are shown in the left and right set of panels, respectively. Statistical uncertainties in the fitted values are indicated by the error bars if larger than the data symbols.

$$b=\exp\left(-\frac{1}{2}q^2R^2\right),$$

$$b=\exp\left[-\frac{1}{2}(q_s^2R_s^2+q_o^2R_o^2+q_l^2R_l^2)\right],$$

$$b=\exp\left[-\frac{1}{2}(q_\perp^2R_\perp^2+q_\parallel^2R_\parallel^2+q_0^2R_0^2)\right]. \tag{3}$$

In Eq. (3) $\boldsymbol{q}=\boldsymbol{p}_1-\boldsymbol{p}_2$ is the three-vector relative momentum, R is the spherical source radius, (q_s,q_o,q_l) and (R_s,R_o,R_l) refer to the three-dimensional, nonspherical source ''side-out-longitudinal'' (SOL) parametrization of Bertsch and Pratt [19], and $(q_\perp,q_\parallel,q_0)$ and $(R_\perp,R_\parallel,R_0)$ refer to the three-dimensional, nonspherical source parametrization of Yano, Koonin, and Podgoretskiĭ [20]. An additional ''out-longitudinal'' cross term [23] in the BP parametrization was not included in this work. The simplified YKP model in the third line of Eq. (3) neglects the longitudinal source velocity, an approximation which should be adequate for collider kinematics near midrapidity. The relative momentum components correspond to the usual definitions where $q_\perp=\sqrt{q_s^2+q_o^2}$, $q_\parallel=q_l$, $q_0=E_1-E_2$, and E_i is the total energy of each particle. For pairs of nonidentical charged particles, e.g., $\pi^+\pi^-$, $C_{2,\mathrm{model}}=G_{\mathrm{Coul}}$ was used.

For the BP and YKP correlation models the chi-square comparison was made using three-dimensional bins in (q_s,q_o,q_l) or $(q_\perp,q_\parallel,q_0)$, respectively. In the figures in the next section, however, three independent, one-dimensional projections are shown where,

$$C_{2,\mathrm{project}}(i)\equiv\frac{N_2^{(B)}}{N_2^{(S)}}\frac{\sum_{j,k}S_2(i,j,k)}{\sum_{j,k}B_2(i,j,k)}, \tag{4}$$

(i,j,k) represent bin labels and include all cyclic permutations of coordinates (q_s,q_o,q_l) or $(q_\perp,q_\parallel,q_0)$, and the sums include those bins containing relative momentum components from 0 to 30 MeV/c. The corresponding projections for the analytical models are given by

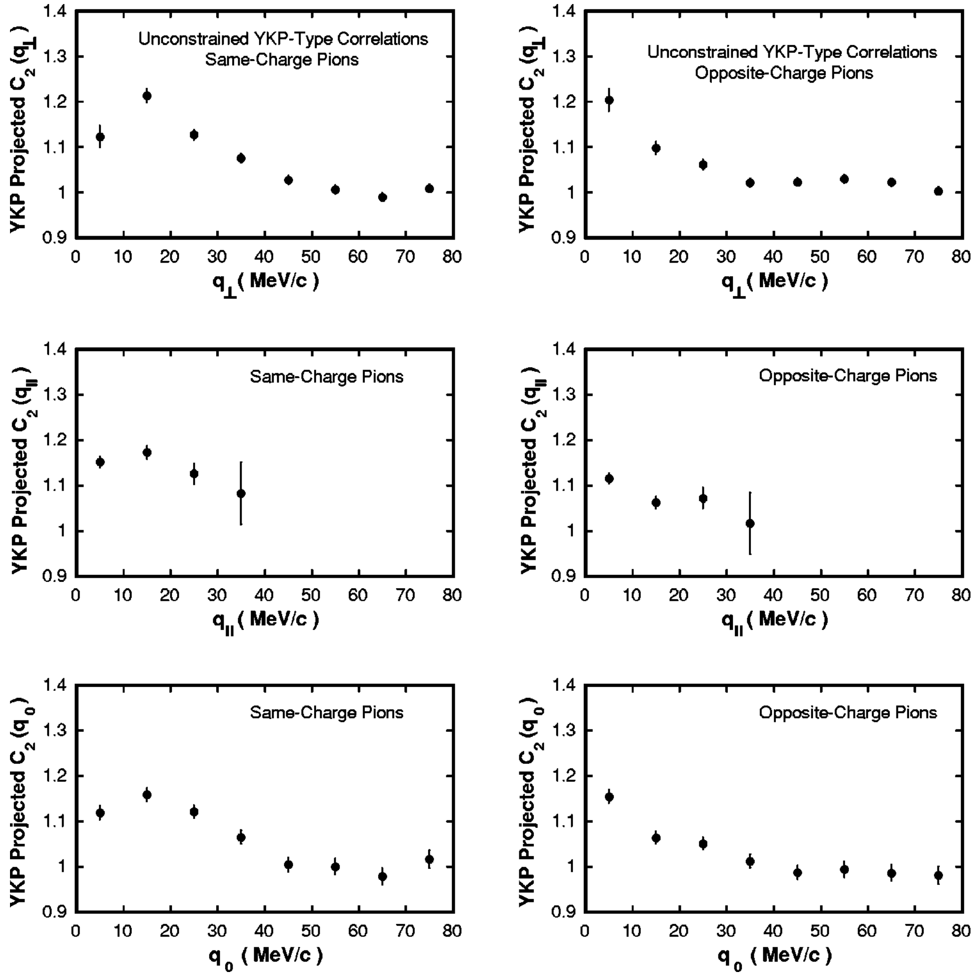

FIG. 5. Three-dimensional YKP two-body, inclusive correlations (solid dots) that result from fitting the one-dimensional $C_2(q)$ correlation function. Projected correlation functions are shown where the statistical uncertainties are indicated by the error bars. Results for the like and unlike charged pion pairs are shown in the left and right set of panels, respectively.

$$C_{2,\text{model project}}(q_i) \equiv \frac{\sum_{j,k} C_{2,\text{model}}(q_i, q_j, q_k) B_2(i,j,k)}{\sum_{j,k} B_2(i,j,k)}, \tag{5}$$

where the momentum components (q_i, q_j, q_k) were evaluated at the centers of the (i,j,k) bins.

Three models for the Coulomb correction G_{Coul} were considered. These correspond to the Gamow factor for point sources [3,4], an empirically modified Gamow correction utilized by NA35 (CERN) [24], and an analytical form obtained by Pratt and Cramer [25] by integrating the Coulomb wave functions over spherical sources for several discrete values of source radii. The latter model was used in the calculations discussed in Secs. III and IV.

Additional capabilities of the HBT simulation model include the following: (1) The computer code can accept the output particle momentum list from any standard relativistic heavy-ion event generator, provided a simple, common data format [26] is used. (2) Correlations for more than two particle types can be generated by repeated application of the processor code to the input particle list. (3) Correlation functions representing more complex source geometries, e.g., expanding sources with radius parameters dependent on $\boldsymbol{K} = \frac{1}{2}(\boldsymbol{p}_1 + \boldsymbol{p}_2)$, can be approximately treated by repeated application of the processor code to the input particle list, where particle pairs whose total momentum $\boldsymbol{K}$ lies within specified kinematic ranges are processed in separate passes. (4) For particle types such as K_S^0 which have relatively low multiplicity per event, the present method fails to produce accurate correlations. However, acceptable correlations may be generated for these particle types by increasing the multiplicity according to a specified one-body distribution using Monte Carlo methods, performing the correlation procedure, then randomly rejecting enough of the particles to reduce the multiplicity back to the original amount.

III. APPLICATION TO RHIC EVENTS

In this section the method is used for high multiplicity, RHIC-like events. A Monte Carlo event generator [27] was used to simulate the π^+ and π^- distributions for 25 200A

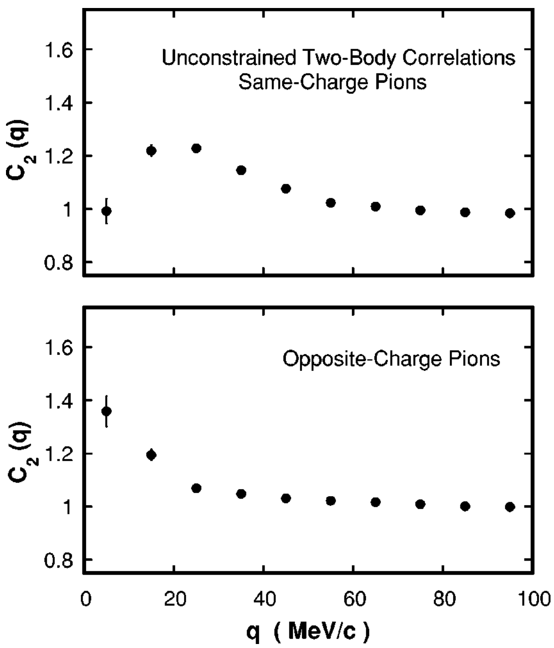

FIG. 6. One-dimensional two-body, inclusive correlations $C_2(q)$ (solid dots) that result from fitting the three-dimensional YKP correlation function. Statistical uncertainties are indicated by the error bars if larger than the data symbols. Results for the like and unlike charged pion pairs are shown in the upper and lower panels, respectively.

GeV Au+Au central events, and the p_T and rapidity (y) pion distributions were made to be consistent with those predicted by VENUS [10]. Azimuthal symmetry was assumed. The (p_T,y) distribution is given by [6]

$$\frac{d^2N}{dp_T dy} = N p_T e^{-m_T/T} e^{-y^2/2\sigma^2}, \tag{6}$$

where N is a normalization factor, $m_T = \sqrt{p_T^2 + m_\pi^2}$ is the transverse mass, m_π is the charged pion rest mass, T is the temperature parameter, and σ is the rapidity width. Fits [28] to the π^+ and π^- distributions predicted by VENUS resulted in parameter values $T=180$ MeV, $\sigma=1.7$ and a combined, mean multiplicity of about 5200 charged pions within the kinematic acceptance region. The latter was taken as $p_T = 0.1-1.0$ GeV/c, $\eta=(-2)-(+2)$, and $\phi=0°-360°$. The (η,ϕ) acceptance and the low p_T cutoff correspond approximately to those of STAR's main tracking detector [21].

The parameters of Eqs. (2) and (3) were assumed to be $R=7$ fm for the one-dimensional model [first line of Eq. (3)], $R_s, R_o, R_l = 6$, 7, and 4 fm, respectively, for the BP three-dimensional model [second line of Eq. (3)], and $R_\perp$, $R_\parallel$, $R_0=6$, 4, and 4 fm, respectively, for the YKP model. For all cases a typical value of $\lambda=0.6$ was used [29]. The finite source size Coulomb correction of Pratt and Cramer [25] with a 9 fm Coulomb source radius was used.

The one-body p_T, η, and ϕ projected distributions were uniformly divided into 50 bins each throughout the respective acceptance ranges. The one-dimensional, two-body correlation distributions were evenly divided into 10 bins from $q=0$ to 100 MeV/c and 2 bins from 100 to 200 MeV/c. For the three-dimensional correlation distributions the regions in (q_s,q_o,q_l) or $(q_\perp,q_\parallel,q_0)$ space from 0 to 80 MeV/c were uniformly divided into an $8\times8\times8$ grid of cubical bins. In addition, a $2\times2\times2$ grid of coarse bins from 0 to 160 MeV/c was used.

The particle momentum adjustment procedure was carried out on an event-by-event basis. The figures to be discussed show only the inclusive quantities for all twenty five events. The inclusive sums of the fitted one-body p_T, η, and ϕ projected spectra are compared with the corresponding reference distributions. The inclusive correlation functions were obtained from Eqs. (1) or (4) by summing the final, fitted S_2 spectra for all twenty five events. The fitted, inclusive correlations are compared with the model values from either Eqs. (2) or (5).

The one-body p_T, η, and ϕ reference distributions served to constrain partially the momentum adjustment procedure as explained in Sec. II. An example of how well the original π^+ and π^- projected distributions were maintained is seen in Fig. 1 for the case in which the one-dimensional $C_2(q)$ model was fitted. The reference projected distributions are indicated by the solid lines where the upper and lower lines indicate the statistical uncertainties in each bin. The fitted distributions are shown by the solid dots (statistical errors are smaller than the data symbols). The fits were done with 50, uniform bins but in Fig. 1 the distributions are plotted using 10 uniform bins in order to enhance the clarity of the figure. Excellent fits such as those displayed in Fig. 1 were routinely obtained.

The fits to the like charge ($\pi^+\pi^+$ and $\pi^-\pi^-$ pairs) and unlike charge ($\pi^+\pi^-$ pairs) one-dimensional correlation functions are shown in Fig. 2. The assumed model values are indicated by the solid lines, and the inclusive, fitted results by the solid dots, where the error bars represent the statistical errors if larger than the data symbols. Quantitative fits to both distributions were readily obtained.

The inclusive fits (solid dots) to the projected, three-dimensional BP model (solid lines) for like and unlike charged pion pairs are shown in Fig. 3. Shown are the q_s, q_o, and q_l projections defined in Eqs. (4) and (5). Statistical uncertainties in the fitted correlations are indicated by the error bars if larger than the data symbols. Quantitative fits to the model correlation functions were readily obtained. Similar results are shown in Fig. 4 for the three-dimensional YKP model, where again we see that quantitative fits were obtained to all six projected correlation functions. The fits to the $q_\parallel$ projection were limited to $q_\parallel < 40$ MeV/c due to poor statistics in bins with larger values of $q_\parallel$.

The computer code was used to generate 1200 π^+ and π^- correlated RHIC-like Au+Au central events for simulation studies by the STAR experiment. On average such computations required about 7.4 CPU minutes per event using a Silicon Graphics Inc. (SGI) Origin 200, 250 MHz processor. This includes the time necessary to generate the reference spectra as well as that needed for 15 – 30 iterations per event.

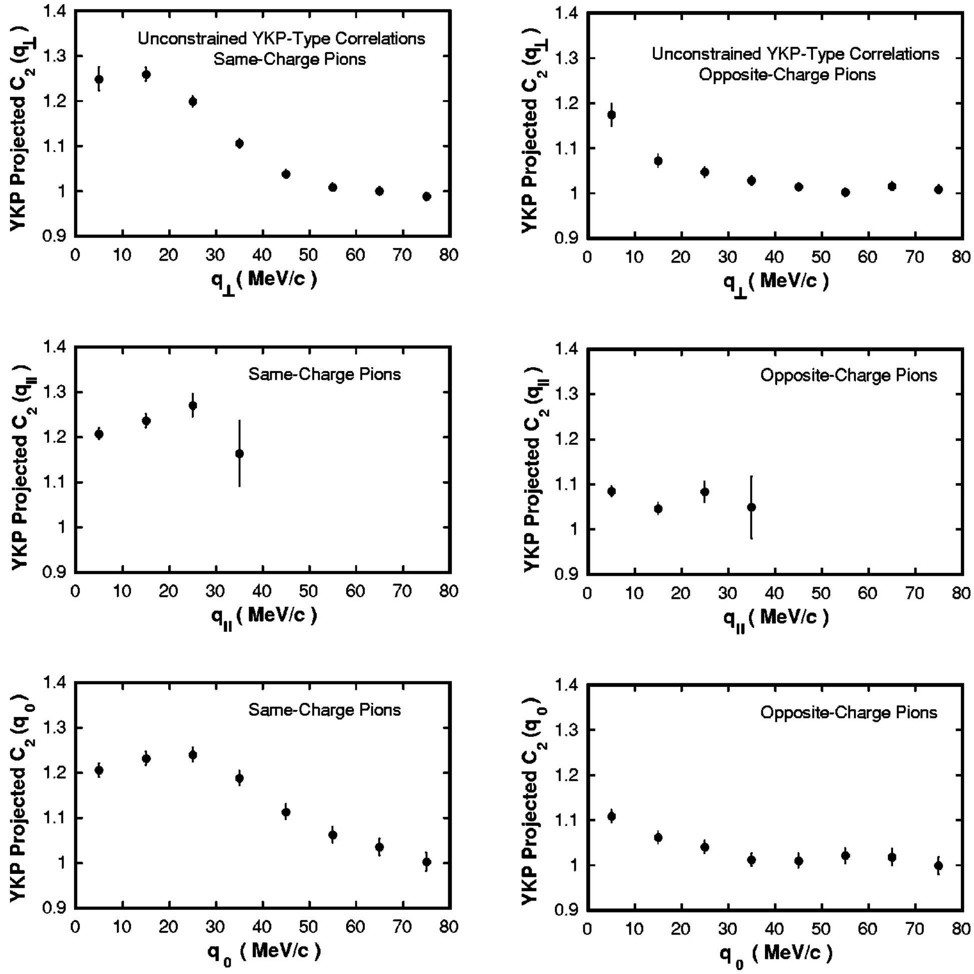

FIG. 7. Three-dimensional YKP two-body, inclusive correlations (solid dots) that result from fitting the three-dimensional BP correlation function. Projected correlation functions are shown where the statistical uncertainties are indicated by the error bars. Results for the like and unlike charged pions are shown in the left and right set of panels, respectively.

IV. UNCONSTRAINED CORRELATIONS

In general, the two-body momentum space correlation function depends on six independent coordinates. Due to statistical limitations for single RHIC-like events, it is only practical to constrain up to three coordinates with the present model. To be useful for simulation studies the generated correlation signals should be robust, i.e., not strongly dependent on the various choices of coordinates which may be selected for study. As long as the correlations in the simulated events are reasonable in strength, range, and shape with respect to different momentum coordinates, then comparison of the input with the final, deduced correlations provides useful information about the performance of the detector and the event reconstruction software.

For example, generating one-dimensional correlations with respect to q should also produce three-dimensional BP correlations of similar strength and range since these coordinates are related by $q^2 = q_s^2 + q_o^2 + q_l^2$. The reverse case should also be true. However, the three-dimensional YKP parametrization additionally depends on $\boldsymbol{K}$ through the $q_0 = |E_1 - E_2|$ term, and, because of this it is not obvious what correlations, if any, will result with respect to the YKP coordinates when the one-dimensional or BP correlations are fitted, and vice versa.

These issues are addressed in this section. The goal is to determine if anomalous or problematic correlation signals are produced, or if correlations vanish, with respect to coordinates which were not explicitly considered in the fitting procedure. No effort was made to relate the BP and YKP parameters [30] other than to select similar source dimensions in both cases. For each case discussed, inclusive correlations are shown for the sample of twenty five events, and only the three independent projections are shown for the three-dimensional correlations.

The YKP correlations that result from fitting the one-dimensional $C_2(q)$ function are shown in Fig. 5 for both like and unlike charged pion pairs. Strong correlations of reasonable shape and range appear in the $q_\perp$ and q_0 projections for both like and unlike pion pairs. Correlations with respect to $q_\parallel$ are present but display irregular shapes and suffer from poor statistics for $q_\parallel > 40$ MeV/c. The same limited range for $q_\parallel$ also occurs for the direct YKP fits (see Fig. 4). The

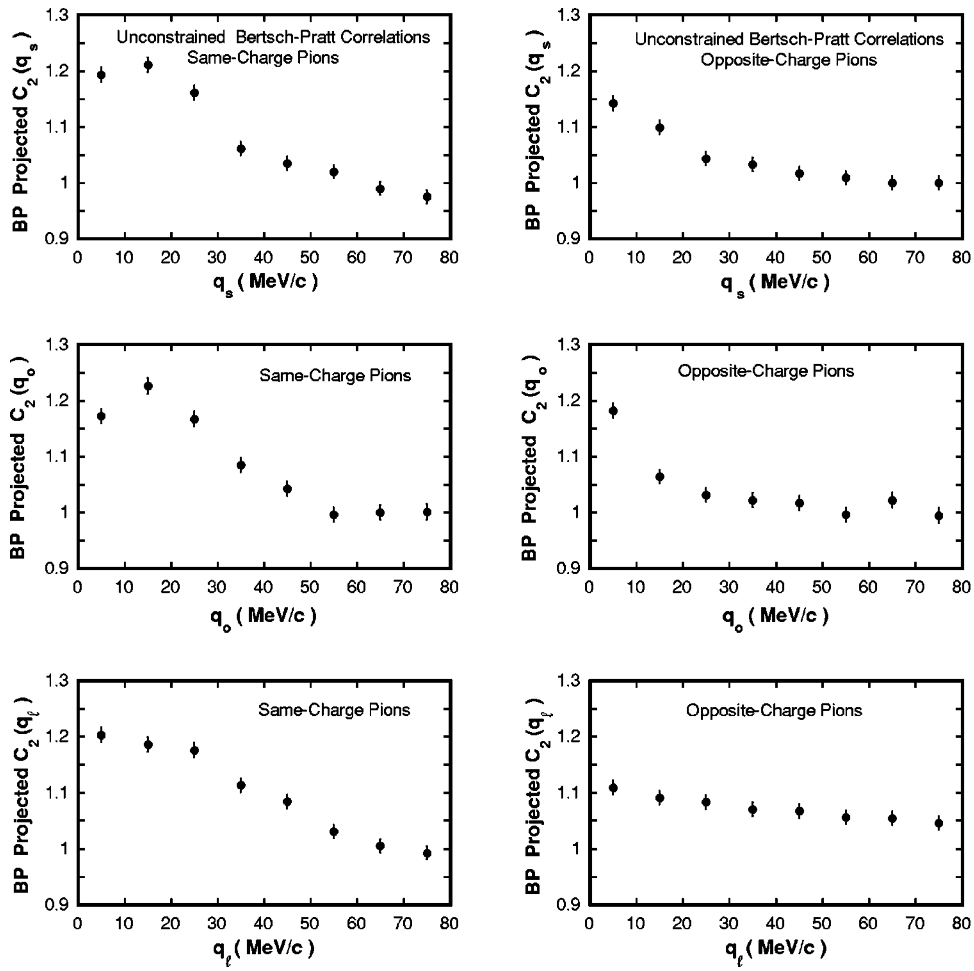

FIG. 8. Three-dimensional side-out-longitudinal BP two-body, inclusive correlations (solid dots) that result from fitting the three-dimensional YKP correlation function. Projected correlation functions are shown where the statistical uncertainties are indicated by the error bars. Results for the like and unlike charged pions are shown in the left and right set of panels, respectively.

one-dimensional $C_2(q)$ correlations that result from fitting the YKP functions are shown in Fig. 6. In this case the correlations are smooth and regular in shape; the repulsive and attractive Coulomb contributions are also quite apparent.

The YKP correlations that result from fitting the BP model are presented in Fig. 7. The correlations with respect to $q_\perp$ are of reasonable strength and range for both the like and unlike pion pairs. The correlations along the $q_\parallel$ axis are reasonable but again suffer poor statistics for $q_\parallel > 40$ MeV/c as was the case in Figs. 4 and 5. The like particle pair correlation with respect to q_0 is of expected magnitude but displays peculiar shape while the unlike particle pair, attractive Coulomb correlation produced along the q_0 axis is reasonable.

The BP correlations that follow from fitting the YKP model are shown in Fig. 8. The correlations with respect to q_s and q_o are of reasonable strength and range for both the like and unlike pion pairs. The correlations for the q_l coordinate are of expected magnitude but that for unlike pairs displays somewhat extended range in momentum space. The latter correlations are, however, consistent with unity in the higher momentum bins from 80 to 160 MeV/c.

V. SUMMARY AND CONCLUSIONS

Detailed understanding of detector performance and event reconstruction efficiency for all of the new RHIC experiments will be required in order to carry out accurate HBT correlation measurements. The simulation model presented here provides the initial step in such a study. A previously reported method for introducing momentum space correlations into the identical particle distributions predicted by relativistic heavy-ion collision event generators was extended considerably in order to provide a practical simulation method for the RHIC experiments. The extensions to the model in Ref. [11] were designed to accommodate the high multiplicities expected at RHIC energies for Au+Au central collision events, to permit the simultaneous correlation of up to two particle types (e.g., π^+ and π^-), to include two commonly used parametrizations for nonspherical source geometries, and to utilize realistic Coulomb corrections appropriate for finite sources.

High quality fits to one- and three-dimensional correlation models for both like and unlike charged pion pairs were obtained for a sample of twenty five simulated VENUS-like, RHIC energy Au+Au central events. The one-body p_T, η, and ϕ projected distributions were constrained, thus approximately imposing total momentum and energy conservation. Two-body correlations were studied with respect to momentum coordinates which were not explicitly constrained by the fitting procedure in order to determine the robustness of the embedded correlation signals. For the most part, these correlations were reasonable in magnitude, range and shape. In conclusion, the present HBT simulation model is well-suited for practical use by the new generation of heavy-ion experiments at RHIC.

ACKNOWLEDGMENTS

The authors are grateful for useful comments and suggestions by Professor John G. Cramer, Jr. (University of Washington), Professor Michael A. Lisa (The Ohio State University), and Dr. Ronald S. Longacre (Brookhaven National Laboratory). This research was supported in part by the U. S. Department of Energy Grant No. DE-FG03-94ER40845 and The Robert A. Welch Foundation.

[1] R. Hanbury Brown and R. Q. Twiss, Philos. Mag. **45**, 633 (1954).
[2] D. H. Rischke and M. Gyulassy, Nucl. Phys. **A608**, 479 (1996).
[3] M. Gyulassy, S. K. Kauffmann, and L. W. Wilson, Phys. Rev. C **20**, 2267 (1979).
[4] D. H. Boal, C.-K. Gelbke, and B. K. Jennings, Rev. Mod. Phys. **62**, 553 (1990).
[5] M.-C. Chu, S. Gardner, T. Matsui, and R. Seki, Phys. Rev. C **50**, 3079 (1994).
[6] T. J. Humanic, Phys. Rev. C **50**, 2525 (1994); **53**, 901 (1996).
[7] R. L. Ray, Phys. Rev. C **57**, 2523 (1998).
[8] S. Pratt, Phys. Lett. B **301**, 159 (1993); Q. H. Zhang, Phys. Rev. C **58**, R18 (1998); **57**, 877 (1998); U. A. Wiedemann, *ibid.* **57**, 3324 (1998); Q. H. Zhang, P. Scotto, and U. Heinz, *ibid.* **58**, 3757 (1998).
[9] X.-N. Wang and M. Gyulassy, Phys. Rev. D **44**, 3501 (1991); **45**, 844 (1992).
[10] K. Werner, Phys. Rep. **232**, 87 (1993).
[11] L. Ray and G. W. Hoffmann, Phys. Rev. C **54**, 2582 (1996).
[12] N. Metropolis, A. W. Rosenbluth, M. N. Rosenbluth, A. H. Teller, and E. Teller, J. Chem. Phys. **21**, 1087 (1953).
[13] S. Pratt *et al.*, Nucl. Phys. **A566**, 103c (1994).
[14] L. Lönnblad and T. Sjöstrand, Eur. Phys. J. C **2**, 165 (1998).
[15] T. Sjöstrand, Comput. Phys. Commun. **82**, 74 (1994).
[16] K. Kadija and P. Seyboth, Phys. Lett. B **287**, 363 (1992).
[17] W. A. Zajc, Phys. Rev. D **35**, 3396 (1987).
[18] W. N. Zhang, Y. M. Liu, L. Huo, Y. Z. Jiang, D. Keane, and S. Y. Fung, Phys. Rev. C **51**, 922 (1995).
[19] G. Bertsch, M. Gong, and M. Tohyama, Phys. Rev. C **37**, 1896 (1988); S. Pratt, T. Csörgő, and J. Zimányi, *ibid.* **42**, 2646 (1990).
[20] F. B. Yano and S. E. Koonin, Phys. Lett. **78B**, 556 (1978); M. I. Podgoretskiĭ, Sov. J. Nucl. Phys. **37**, 272 (1983).
[21] J. W. Harris *et al.*, STAR Collaboration, Nucl. Phys. **A566**, 277c (1994).
[22] K. Kadija, NA49 Collaboration, Nucl. Phys. **A610**, 248c (1996); H. Appelshäuser *et al.*, NA49 Collaboration, Eur. Phys. J. C **2**, 661 (1998).
[23] S. Chapman, P. Scotto, and U. Heinz, Phys. Rev. Lett. **74**, 4400 (1995); J. Barrette *et al.*, E877 Collaboration, *ibid.* **78**, 2916 (1997).
[24] T. Alber *et al.*, NA35 Collaboration, Z. Phys. C **73**, 443 (1997).
[25] S. Pratt, computer codes PIPIBIG and PIPIPM (unpublished); PIPIPM modified and results tabulated by J. G. Cramer (unpublished); J. G. Cramer (private communication).
[26] P. Jacobs and D. Irmscher, STAR Collaboration, STAR Note No. 235, 1996 (unpublished).
[27] R. L. Ray, computer code MULTGEN (unpublished).
[28] R. S. Longacre (private communication).
[29] I. G. Bearden *et al.*, NA44 Collaboration, Phys. Rev. C **58**, 1656 (1998).
[30] U. Heinz, B. Tomášik, U. A. Wiedemann, and Y.-F. Wu, Phys. Lett. B **382**, 181 (1996).